Optical binding forces between plasmonic nanocubes: A numerical study based on discrete-dipole approximation*

Zhang Xiao-Ming(张小明), Xiao Jun-Jun(肖君军)†, and Zhang Qiang(张 强)

College of Electronic and Information Engineering, Shenzhen Graduate School, Harbin Institute of Technology, Shenzhen 518055, *China*

(Received 14 May 2013; revised manuscript received 26 June 2013; published 3 December 2013)

Plasmonic nanocubes are ideal candidates in realizing controllable reflectance surfaces, unidirectional nanoantennas and other plasmon-associated applications. In this work, we perform full-wave calculations of the optical forces in three-dimensional gold nanocube dimers. For a fixed center-to-center separation, the rotation of the plasmonic nanocube leads to a slight shift of the plasmonic resonance wavelength and a strong change in the optical binding forces. The effective gap and the near field distribution between the two nanocubes are shown to be crucial to this force variation. We further find that the optical binding force is dominated by the scattering process while the optical forces in the wavevector direction are affected by both scattering and absorption, making the former relatively more sensitive to the rotation of (an effective gap between) the nanocubes. Our results would be useful for building all-optically controllable meta-surfaces.

Keywords: optical binding force, nanocube dimer, surface plasmon resonance

PACS: 73.20.Mf, 78.67.Bf, 42.50.Wk, 78.68.+m **DOI:** 10.1088/1674-1056/23/1/017302

1. Introduction

Plasmonic nanostructures have attracted much attention due to their remarkable optical properties associated with surface plasmons, enabling applications in bio-chemical sensing,[1] high-resolution imaging,[2] deep subwavelength waveguiding[3] and surface enhanced spectroscopy,[4] etc. Fundamentally, these phenomena are due to the propagating surface plasmon polaritons or the localized surface plasmon resonance (LSPR). Various kinds of plasmonic nanostructures supporting the LSPR have been investigated, including nanospheres, nanoshells, nanopillars, nanorings, as well as their aggregates, providing an amount of degrees of freedom to control the optical fields temporally, spatially and spectrally.[5] Plasmonic nanoparticles (e.g., gold and silver) therefore represent a promising class of nanomatericals for LSPR related applications. They can be routinely fabricated by top-down lithography methods or synthesized in a bottom-up scheme, resulting in a variety of well-defined and controllable sizes, shapes and morphologies.[1] Plasmon resonances lead to relatively large optical cross sections and extremely strong localized near fields at specific wavelengths.[6–8] Near the resonant point, the mutual optical forces between the nanoparticles are dramatically enhanced and can be used to control the relative positions of the nanoparticles, enabling a tunable structural design for photovoltaic and sensing purposes.[9,10] In such a vein, theoretical researches for the optical forces in plasmonic systems and optically bound clusters can be of great help.[11–13]

Very recently, a plasmonic nanocube colloid coupled to a metallic substrate was shown to work as an anti-reflective meta-surface.[14] The surface coverage of the nanocubes is not crucial as long as they are randomly dispersed. However, the nanocube morphology (e.g., dimerization, clustering and edge rounding) could be critical due to the coupled plasmon resonances which may deteriorate the gap-plasmon-guided modes. The inter-nanocube distance, the relative nanocube orientation and the surface curvature can affect the plasmonic properties since they finely control the effective capacitance of the two facing metallic surfaces and the resulting electrostatic coupling between the surface charge distributions. In this regard, it is possible to assemble nanocubes into an array by optical binding forces and to manipulate the bonding and antibonding hybridized plasmon modes. Based on that, we envision a possibility of an all-optically controllable meta-surface.

In terms of modeling optical forces, the multiple scattering theory is basically the most accurate tool for spherical particles and their clusters.[15] However, it is not applicable to more complex geometries (e.g., rods, cubes and stars), for which we shall employ a more general electrodynamics approach. To calculate the optical forces, we adopt the discrete dipole approximation (DDA) method[16–22] to obtain the electromagnetic fields and then use the summation of Lorentz forces or the closed-surface integration of the Maxwell stress tensor.[12,13] In such, our numerical schemes are applicable to arbitrarily shaped particles under arbitrary incident optical fields. We provide a detailed investigation of the optical forces of a gold nanocube dimer (see inset of Fig. 1(a)) with different geometrical configurations (e.g., relative orientations and gap distances). These results would help to understand and guide

*Project supported by the National Natural Science Foundation of China (Grant Nos. 11004043, 11274083, and 61107036) and the SZMSTP, China (Grant Nos. JC201005260185A, JCYJ20120613114137248, 2011PTZZ048, JC201105160524A, and KQCX20120801093710373).

†Corresponding author. E-mail: eiexiao@hitsz.edu.cn

© 2014 Chinese Physical Society and IOP Publishing Ltd

a broad range of experimental studies.

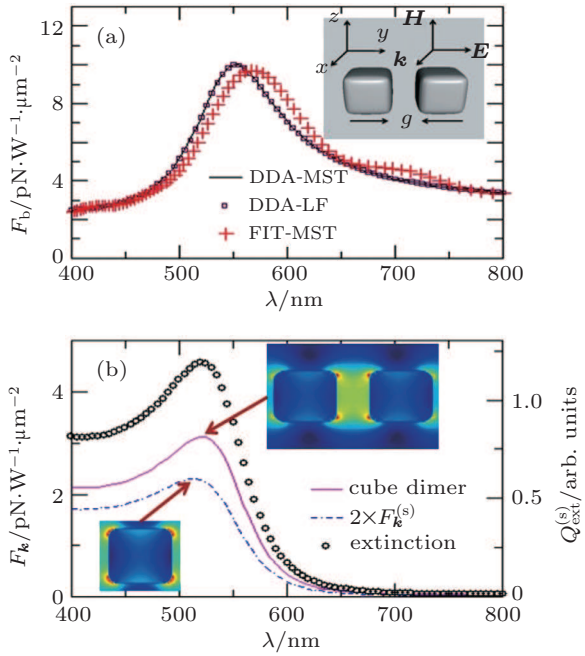


Fig. 1. (color online) The optical force spectra for a nanocube dimer and a single nanocube. (a) Optical binding forces between the two nanocubes calculated by three different numerical methods (DDA-MST, DDA-LF and FIT-MST). (b) Optical forces along the $\boldsymbol{k}$ direction for a single nanocube and the nanocube dimer. Inset in panel (a) shows the geometry of the plasmonic dimer consisting of two identical nanocubes. The sharp edges of the cube (length $L = 20$ nm) are replaced by quarter cylinders of radius 4 nm, which are set tangential to the cube faces. The face-to-face gap distance is $g = 10$ nm in this case.

2. Numerical methods and benchmark

One of the main ingredients of the DDA is the replacement of an object by dipoles in an orthogonal grid. Once the dipole polarizabilities α_j are specified, for a monochromatic incident plane wave, each dipole is affected by the incident wave and the electric field at this dipole location due to all the other point dipoles, as dictated by the coupled-dipole equations[15–17]

$$\boldsymbol{E}_i = \boldsymbol{E}_i^{\text{inc}} - \sum_{i\neq j} A_{ij}\cdot\boldsymbol{P}_j, \tag{1}$$

where $\boldsymbol{P}_j = \alpha_j\boldsymbol{E}_j$ represents the polarization of dipole j and $-A_{ij}\boldsymbol{P}_j$ is the electric field at $\boldsymbol{r}_i$ due to dipole $\boldsymbol{P}_j$ at location $\boldsymbol{r}_j$. The A_{ij} is a 3×3 matrix given by

$$A_{ij} = \frac{\exp(\mathrm{i}kr_{ij})}{r_{ij}}\times\left[k^2(\hat{\boldsymbol{r}}_{ij}\hat{\boldsymbol{r}}_{ij}-\boldsymbol{I}) + \frac{\mathrm{i}kr_{ij}}{r_{ij}^2}(3\hat{\boldsymbol{r}}_{ij}\hat{\boldsymbol{r}}_{ij}-\boldsymbol{I})\right], \quad \text{for } i\neq j, \tag{2}$$

where $r_{ij} = |\boldsymbol{r}_i - \boldsymbol{r}_j|$, $\hat{\boldsymbol{r}}_{ij} = (\boldsymbol{r}_i - \boldsymbol{r}_j)/r_{ij}$, $k = |\boldsymbol{k}|$ is the magnitude of the wave vector and $\boldsymbol{I}$ is the 3×3 identity matrix. When $i = j$, we define $A_{jj} = \alpha_j^{-1}$. Once all $\boldsymbol{P}_j$ are obtained by Eq. (1), the electromagnetic field at any location can be calculated similarly.[17]

There are then basically two approaches for calculating the optical forces on the object. The first one is by the summation of the Lorentz forces, which after being time averaged reads[15]

$$\boldsymbol{F} = \frac{1}{2}\mathrm{Re}[(\boldsymbol{P}^*\cdot\boldsymbol{\nabla})\boldsymbol{E} + \mathrm{i}k\boldsymbol{P}^*\times\boldsymbol{B}], \tag{3}$$

where $\boldsymbol{E}$ and $\boldsymbol{B}$ are the total electric and magnetic fields acting on dipole $\boldsymbol{P}$. In Eq. (3), the asterisk denotes the complex conjugation. It is important to stress that the spatial derivatives do not include contributions resulting from the changes in dipole moments due to the displacements of particles. In an assembly of nanoparticles, we can sum over the appropriate subsets of the entire dipole array belonging to each object/nanoparticle respectively, obtaining the optical force vector. This scheme is referred to as the DDA plus Lorentz force (DDA-LF) method.

We can also calculate the optical force acting on a given particle by evaluating the vector flux of the Maxwell stress tensor over a surface surrounding that particle[11–13]

$$\boldsymbol{F} = \oiint_S \langle\boldsymbol{T}\rangle\cdot\hat{\boldsymbol{n}}\,\mathrm{d}s, \tag{4}$$

where the time averaged Maxwell stress tensor is given by

$$\langle\boldsymbol{T}\rangle = \frac{1}{2}\mathrm{Re}\left[\varepsilon\varepsilon_0\boldsymbol{E}\boldsymbol{E}^* + \mu\mu_0\boldsymbol{H}\boldsymbol{H}^* - \frac{\boldsymbol{I}}{2}(\varepsilon\varepsilon_0|\boldsymbol{E}|^2 + \mu\mu_0|\boldsymbol{H}|^2)\right]. \tag{5}$$

Here, ε, μ are the relative permittivity and permeability of the background material, respectively. This scheme using Eqs. (4) and (5) to obtain the optical force is called the DDA plus Maxwell stress tensor (DDA-MST) method. To justify the accuracy of our force calculations by the two approaches DDA-LF and DDA-MST, we have compared the results to the ones by a finite-integral technique plus MST (FIT-MST),[12] as shown in Fig. 1(a) for a pair of nanocubes that are placed nearby. In all DDA-based simulations, the inter-dipole separation is kept constant at around 0.56 nm, yielding a total of 48000 dipoles per nanocube. The incident radiation propagates along the $\hat{x}$ axis and is polarized along the $\hat{y}$ axis (i.e., parallel to the axis of the dimer). The dielectric functions of the gold nanoparticle are modeled with a modified Drude form that is fitted to the experimental data.[12,13] The surrounding medium is assumed to be the vacuum. Good agreements of the results by the three methods (DDA-LF, DDA-MST and FIT-MST) are seen for the optical binding force F_b, which is defined as the $\hat{y}$ component of the difference between the total forces acting upon each nanocube. Especially, the spectra of the optical binding forces calculated by DDA-MST and the DDA-LF almost completely match. Note that there are small deviations between the DDA-LF and the FIT-MST results, which are due to numerical errors. This can occur for

different reasons. Firstly, the FIT is a time-domain algorithm while the DDA is a frequency-domain one. Secondly, the total number of meshes, the bandwidth of the incident pulse, the size of the box for the MST integration and the postprocessing electromagnetic field calculation can all lead to some numerical errors.

3. Results and discussion

3.1. Optical forces on normal cube dimers of different gaps

With the DDA-based methods, we have studied the optical forces in a series of nanocube dimers. In Fig. 1(b), we plot both the extinction cross section $Q_{\rm ext}^{(\rm s)}$ (circles) of a single nanocube and the $\boldsymbol{k}$-direction force $F_{\boldsymbol{k}}$ (thin solid line) for a nanocube dimer that is in a face-to-face configuration with gap $g = 10$ nm (see the inset of Fig. 1(a)). It is seen that the $\boldsymbol{k}$-direction optical force (e.g., optical pressure) spectrum of the nanocube dimer has a line shape similar to its extinction cross section efficiency. This is a consequence of the usual radiation pressure, which is basically determined by the extinction cross section and the differential cross section distribution.[18] The optical scattering forces $F_{\boldsymbol{k}}^{(\rm s)}$ of a single cube rotated along the different axes with respect to the $\boldsymbol{k}$ direction have a nearly identical profile (figures not shown here), which indicates that the orientation has a weak effect of the optical force on a single cubic particle.

However, when the coupled plasmon resonances take place, the near-field enhancement is numerous in the gap region (see the inset of Fig. 1(b)) and the resonant optical spectrum is altered. For comparison, the doubled $\boldsymbol{k}$-direction force $F_{\boldsymbol{k}}^{(\rm s)}$ of an isolated nanocube is also plotted (dash-dotted line) in Fig. 1(b). It is seen that putting two nanocubes close to each other can enhance the $\boldsymbol{k}$-direction optical force $F_{\boldsymbol{k}}$. This is mainly due to the coupled plasmon resonances induced by the dimerization effect. By this, it is expected that the mutual interacting optical force between the two nanocubes could become highly anisotropic. As shown in Fig. 2, for gap distance g varying from 6 nm to 30 nm, the optical force spectra depend strongly on the gap between the cubes. The magnitudes of the optical forces (both $F_{\rm b}$ and $F_{\boldsymbol{k}}$) increase as the inter-particle distance g is decreased. This is partially because the interaction between the metallic cubes and the local electromagnetic field becomes stronger as the gap decreases.[13,15]

A subtle difference between Figs. 2(a) and 2(b) is that the peak positions of the $F_{\rm b}$ spectra remain nearly unchanged but the ones of the $F_{\boldsymbol{k}}$ spectra are slightly blue-shifted as the dimer gap increases. For the longitudinal excitation, the gap g (6–30 nm) is much smaller than the excitation wavelength (400–800 nm), which is also quite larger than the size of the nanocube (20 nm×20 nm × 20 nm). A simple dipole–dipole model satisfactorily explains the $F_{\boldsymbol{k}}$ spectra of the coupled plasmons and the plasmon resonance blue-shifts when the gap increases.[15] In the system we studied, the absorption surpasses the scattering. We further notice that $F_{\boldsymbol{k}}$ is contributed by both the scattering and absorption processes of photons. However, the binding force is more related to the pure scattering process and has not much correlation with the photon absorption. This is also reflected by the line shapes in Fig. 2: the curves of optical binding forces $F_{\rm b}$ are rather symmetrical around the resonances; however, the curves of optical scattering forces $F_{\boldsymbol{k}}$ are nonsymmetric due to the larger absorption coefficients of gold at high frequencies caused by the interband transition.[14] As a matter of fact, optical binding is a type of light-matter interaction between small particles that is mediated by the light re-scattering by the particles.[15] In other words, the curve shape of $F_{\boldsymbol{k}}$ is very close to that of the extinction cross section, while the curve of the optical binding force $F_{\rm b}$ does not show a similar shape.

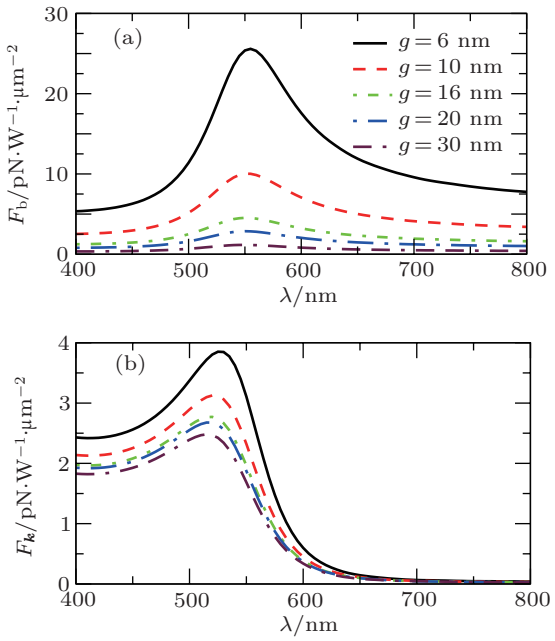


Fig. 2. (color online) Optical force spectra for nanocube dimers with different gaps: (a) optical forces between cubes, (b) optical forces along the $\boldsymbol{k}$ direction of the incident wave.

3.2. Optical forces of rotated cube dimers

In a collection of samples, the nanocubes may have different orientations[14] and the face-to-face configuration discussed in the previous section may only be a special case. To characterize a more general nanocube pair, we can rotate the cube along the z axis with an angle θ (see the inset of Fig. 1(a)). Figure 3 shows respectively the optical binding force $F_{\rm b}$ and the $\boldsymbol{k}$-direction force $F_{\boldsymbol{k}}$ for face-to-face, face-to-edge and edge-to-edge configurations with a fixed surface-to-surface gap distance. It is seen that with the same g, the force has the maximum amplitude when the two nanocubes are oriented in the face-to-face configuration. The resonant

frequency does not shift much as one nanocube is rotated with respect to the other. However, the effective surface-to-surface gap between the nanocubes is increased when θ increases from 0° to 45°. Correspondingly, the extinction and scattering cross sections are shown in Fig. 4 for the three configurations. The bold yellow lines in the subfigures are the doubled optical cross sections (i.e., $2Q_{\rm ext}^{(\rm s)}$ and $2Q_{\rm sca}^{(\rm s)}$) of a single nanocube. The results show that pulling the two naocubes closer can enhance the total extinction cross section, which exceeds the $2Q_{\rm ext}^{(\rm s)}$ and $2Q_{\rm sca}^{(\rm s)}$ curves. This is particularly true for the scattering cross sections, as shown in Figs. 4(b) and 4(d). This feature also explains the observation in Fig. 3 that $F_{\rm b}$ is more dramatically affected than $F_{\boldsymbol{k}}$ when the effective surface-to-surface gap is varied by rotating the nanocube(s).

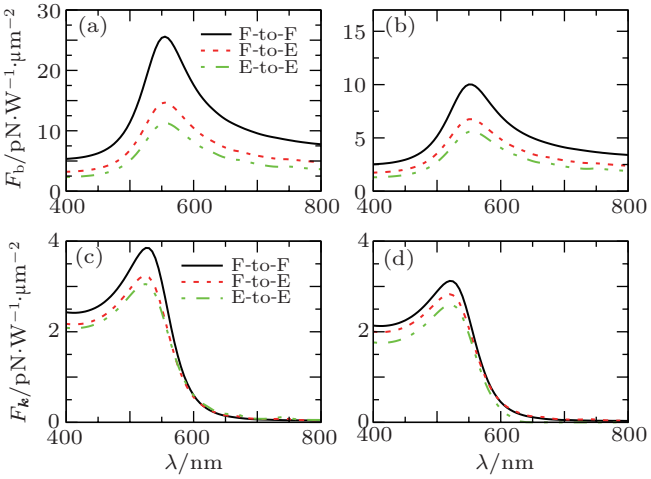


Fig. 3. (color online) Optical forces for three different configurations (face-to-face, face-to-edge and edge-to-edge). (a) and (c) The optical binding forces and total scattering forces along the $\boldsymbol{k}$ direction when $g = 6$ nm. (b) and (d) The optical force spectra for fixed $g = 10$ nm.

Since the nanocubes we used in this study are rather small (e.g., edge length $L = 20$ nm), it is reasonable that the extinction cross section is dominated by the absorption, as scattering contributes around 1% (see the scales in Fig. 4). By such, the plasmon resonant position in the spectrum is nearly stabilized at $\lambda = 545$ nm for the various orientations. The near field distributions at this wavelength are shown in Fig. 5 for several typical cases. The near-field variations are noticeable in both pattern and hot spots, which we believe lead to the strong variations in the optical binding force $F_{\boldsymbol{k}}$.

To demonstrate the force dependence on the relative orientation of the two nanocubes more specifically, we show in Fig. 6 a series of results for the optical forces when the rotation angle of one nanocube gradually varies ($\theta = 0°$, 10°, 20°, 30°, 45°). We keep the other nanocube untouched and the center-to-center distance fixed at $d = 30$ nm. It is seen that the magnitudes of the forces are increased correspondingly. However, for the same amount of rotation angle, $F_{\rm b}$ changes more

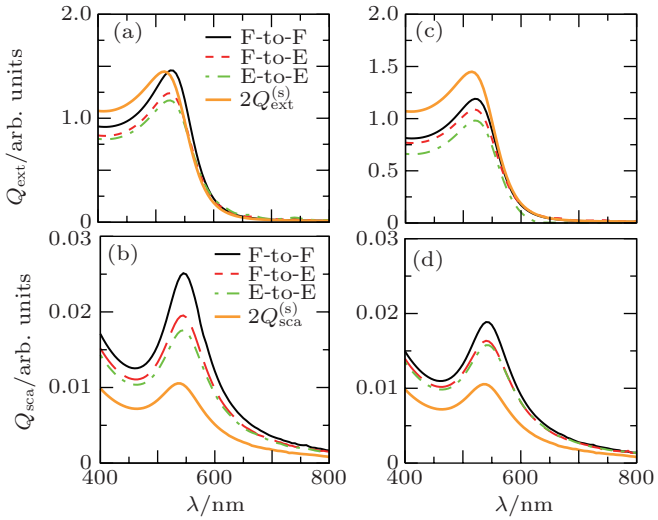


Fig. 4. (color online) Optical cross sections for the three different configurations. (a) Extinction cross section and (b) total scattering cross section for $g = 6$ nm. Panels (c) and (d) show the optical cross sections for $g = 10$ nm.

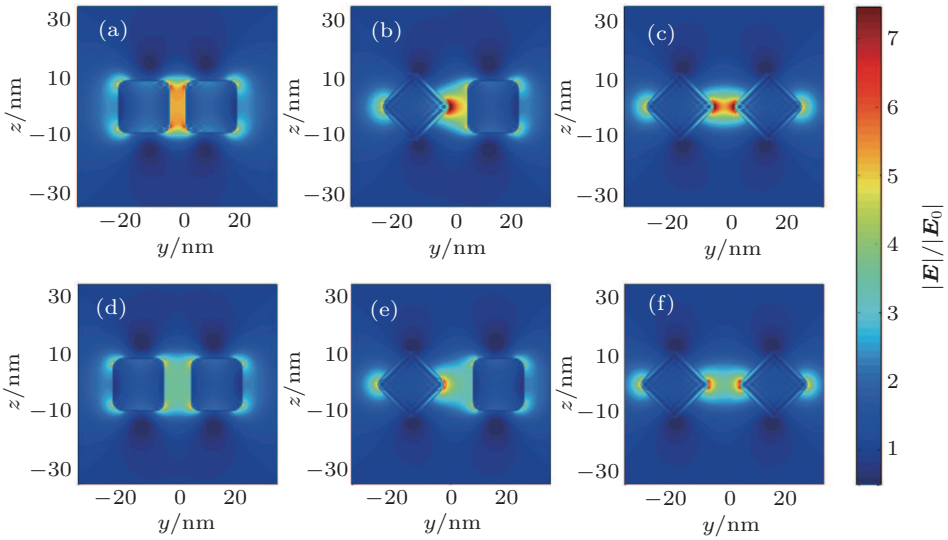


Fig. 5. (color online) Near-field distribution $|\boldsymbol{E}/\boldsymbol{E}_0|$ across the yz plane at the plasmon resonance of $\lambda = 545$ nm. Top panels (a)–(c) are for gap distance $g = 6$ nm and bottom panels (d)–(f) are for $g = 10$ nm.

dramatically than $F_{\boldsymbol{k}}$ does. It is interesting that the peak position of the binding force spectrum remains nearly unchanged when the rotation angle θ is changed. However, the peak position of the scattering force spectrum has a slightly redshift when θ increases gradually. We believe that these results can also be attributed to the previous reasoning that the binding force is dominated by the scattering process.

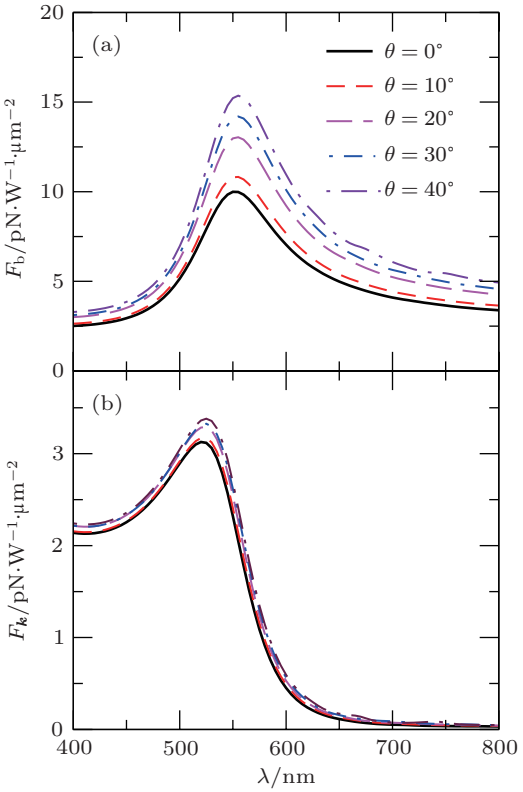


Fig. 6. (color online) Spectra of optical forces for one nanocube rotating along the z axis: (a) binding forces $F_{\rm b}$ between the cubes, (b) total scattering force $F_{\boldsymbol{k}}$.

4. Conclusion

We implement and benchmark a full wave optical force calculation method for three-dimensional arbitrary shaped objects based on the discrete dipole approximation. We then apply it to study the optical forces in gold nanocube dimers. It is found that the mutual plasmon interaction between the nanocubes can lead to enhanced optical forces with respect to a single nanocube. The optical binding force is essentially dominated by the scattering process while the scattering force along the incident wave vector is more closely correlated to the total extinction efficiency. This may explain the observation that the optical binding force is more sensitive to the effective surface-to-surface gap distance of the dimer. Our results could be useful in building an all-optically controllable surface that couples the nanocubes to a metal film.

References

[1] Chen H J, Shao L, Li Q and Wang J F 2013 *Chem. Soc. Rev.* **42** 2679
[2] Wu X, Ming T, Wang X, Wang P N, Wang J F and Chen J Y 2010 *ACS Nano* **4** 113
[3] Chen H Y, He C L, Wang C Y, Lin M H, Mitsui D, Eguchi M, Teranishi T and Gwo S 2011 *ACS Nano* **5** 8223
[4] Svedberg F, Li Z, Xu H and Käll M 2006 *Nano Lett.* **6** 2639
[5] Gandra N, Abbas A, Tian L and Singamaneni S 2012 *Nano Lett.* **12** 2645
[6] Chen H J, Sun Z H, Ni W H, Woo K C, Lin H Q, Sun L D, Wang J F and Yan C H 2009 *Small* **5** 2111
[7] Prodan E, Radloff C, Halas N and Nordlander P 2003 *Science* **302** 419
[8] Amendola V, Bakr O M and Stellacci F 2010 *Plasmonics* **5** 85
[9] Wang X, Xiao K, Min C, Zou Q, Hua Y and Yuan X C 2013 *Plasmonics* **8** 637
[10] Yan Z, Shah R A, Garrett Chado, Gray S K, Pelton M and Scherer N F 2013 *ACS Nano* **7** 1790
[11] Xiao J J, Zheng H H, Sun Y X and Yao Y 2010 *Opt. Lett.* **35** 962
[12] Zhang Q, Xiao J J, Zhang X M and Yao Y 2013 *Opt. Express* **21** 6601
[13] Zhang Q, Xiao J J, Zhang X M and Yao Y 2013 *Opt. Commun.* **301–302** 121
[14] Moreau A, Ciracì C, Mock J J, Hill R T, Wang Q, Wiley B J, Chilkoti A and Smith D R 2012 *Nature* **492** 86
[15] Miljkovic V D, Pakizeh T, Sepulveda B, Johansson P and Kall M 2010 *J. Phys. Chem. C* **114** 7472
[16] Draine B T and Flatau P J 1994 *J. Opt. Soc. Am. A* **11** 1491
[17] Evlyukhin A B, Reinhardt C and Chichkov B N 2011 *Phys. Rev. B* **84** 235429
[18] Xiao J J and Chan C T 2008 *J. Opt. Soc. Am. B* **25** 1553
[19] Zhou F, Liu Y and Li Z Y 2011 *Chin. Phys. B* **20** 037303
[20] Hoekstra A G, Frijlink M, Waters L B F M and Sloot P M A 2001 *J. Opt. Soc. Am. A* **18** 1944
[21] Chaumet P C and Nieto-Vesperinas M 2000 *Phys. Rev. B* **61** 14119
[22] Karásek V, Brzobohatý O and Zemánek P 2009 *J. Opt. A: Pure Appl. Opt.* **11** 034009